

## Dynamics of Mitochondrial RNA-Binding Protein Complex in *Trypanosoma brucei* and Its Petite Mutant under Optimized Immobilization Conditions

Zhenqiu Huang, Sabine Kaltenbrunner, Eva Simková, David Stanek, Julius Lukes and Hassan Hashimi  
*Eukaryotic Cell* 2014, 13(9):1232. DOI: 10.1128/EC.00149-14.  
Published Ahead of Print 25 July 2014.

---

Updated information and services can be found at:  
<http://ec.asm.org/content/13/9/1232>

---

**SUPPLEMENTAL MATERIAL**

*These include:*

[Supplemental material](#)

**REFERENCES**

This article cites 37 articles, 20 of which can be accessed free at: <http://ec.asm.org/content/13/9/1232#ref-list-1>

**CONTENT ALERTS**

Receive: RSS Feeds, eTOCs, free email alerts (when new articles cite this article), [more»](#)

---

---

Information about commercial reprint orders: <http://journals.asm.org/site/misc/reprints.xhtml>  
To subscribe to to another ASM Journal go to: <http://journals.asm.org/site/subscriptions/>

---

# Dynamics of Mitochondrial RNA-Binding Protein Complex in *Trypanosoma brucei* and Its Petite Mutant under Optimized Immobilization Conditions

Zhenqiu Huang,<sup>a,b</sup> Sabine Kaltenbrunner,<sup>b</sup> Eva Šimková,<sup>c</sup> David Staněk,<sup>c</sup> Julius Lukeš,<sup>a,b</sup> Hassan Hashimi<sup>a,b</sup>

Institute of Parasitology, Biology Centre, Czech Academy of Sciences, České Budějovice (Budweis), Czech Republic<sup>a</sup>; Faculty of Sciences, University of South Bohemia, České Budějovice (Budweis), Czech Republic<sup>b</sup>; Institute for Molecular Genetics, Czech Academy of Sciences, Prague, Czech Republic<sup>c</sup>

There are a variety of complex metabolic processes ongoing simultaneously in the single, large mitochondrion of *Trypanosoma brucei*. Understanding the organellar environment and dynamics of mitochondrial proteins requires quantitative measurement *in vivo*. In this study, we have validated a method for immobilizing both procyclic stage (PS) and bloodstream stage (BS) *T. brucei* with a high level of cell viability over several hours and verified its suitability for undertaking fluorescence recovery after photobleaching (FRAP), with mitochondrion-targeted yellow fluorescent protein (YFP). Next, we used this method for comparative analysis of the translational diffusion of mitochondrial RNA-binding protein 1 (MRP1) in the BS and in *T. b. evansi*. The latter flagellate is like petite mutant *Saccharomyces cerevisiae* because it lacks organelle-encoded nucleic acids. FRAP measurement of YFP-tagged MRP1 in both cell lines illuminated from a new perspective how the absence or presence of RNA affects proteins involved in mitochondrial RNA metabolism. This work represents the first attempt to examine this process in live trypanosomes.

The kinetoplastid flagellates belonging to the *Trypanosoma brucei* group have been a focus of research because they are etiological agents of human African trypanosomiasis, a serious disease commonly referred to as sleeping sickness, which is spread among humans and large mammals by the *Glossina* fly in sub-Saharan Africa. Yet, *T. brucei* has also emerged as a powerful model for eukaryotic cell biology as efforts to understand it as a pathogen have revealed many fascinating biological properties. For example, its simple cell architecture (1) has been exploited to understand organelle biogenesis (2, 3).

The single, large mitochondrion of *T. brucei* has also become known for a number of divergent characteristics that have been a subject of intense research (4). Its mitochondrial genome, called kinetoplast DNA (kDNA), is a compact network composed of thousands of the mutually concatenated DNA minicircles and maxicircles adjacent to the flagellar basal body. Many of the protein-coding genes located on the kDNA maxicircles require extensive RNA editing of the uridine (U) insertion and/or deletion type, eventually yielding translatable open reading frames (ORFs). Small noncoding transcripts called guide RNAs (gRNAs), encoded almost exclusively by the minicircles, provide the information for each U insertion/deletion event via binding to its cognate mRNA. The resulting proteins are involved in mitochondrial respiratory complexes and translation. During its life cycle, the mitochondrion of *T. brucei* undergoes a transition from the large, reticulated organelle of the insect midgut-dwelling procyclic stage (PS), which is equipped with the electron transport chain complexes, to a morphologically reduced organelle devoid of cristae, which is characteristic for the glycolysis-dependent slender bloodstream stage (BS) that infects mammalian hosts (1, 5).

Live-cell imaging is increasingly employed to study eukaryotic cellular function, enabling real-time tracking of biological processes of individual cells. Advanced microscopy techniques such as fluorescence recovery after photobleaching (FRAP), fluorescence correlation spectroscopy (FCS), and fluorescence resonance

energy transfer (FRET) can provide informative and critical insights into protein dynamics such as diffusion, assembly, and interaction with partners (6). In order to apply these powerful techniques to *T. brucei* and other flagellates, the vigorous motility of these cells must be accommodated (7), calling into need techniques that efficiently immobilize cells yet maintain them in an appropriate physical state.

Immobilization of the BS on agarose has been employed to study apolipoprotein L1-mediated lysis and mitochondrial membrane potential in live cells (8, 9). The PS flagellates have been embedded in low-melting-point agarose to study Golgi compartment duplication and bilobe protein turnover (10) or sandwiched between a slide and a coverslip to examine intraflagellar transport by FRAP (11). While these methods were utilized to great effect in their respective studies, the influence of the immobilization techniques on cell viability was not specifically addressed. A study in which kinetoplastid protists were immobilized in a CyGEL matrix did systematically assay cell viability, claiming its suitability for the PS and *Leishmania major* but not for the BS (12). This immobilization method was later used to study the trafficking of surface proteins in *L. major* by FRAP (13).

Here, we describe a rapid, economical, and reproducible immobilization method that can be used with an inverted microscope and compensates for the absence of a dedicated chamber for

Received 21 June 2014 Accepted 21 July 2014

Published ahead of print 25 July 2014

Address correspondence to Julius Lukeš, jula@paru.cas.cz, or Hassan Hashimi, hassan@paru.cas.cz.

Supplemental material for this article may be found at <http://dx.doi.org/10.1128/EC.00149-14>.

Copyright © 2014, American Society for Microbiology. All Rights Reserved.  
doi:10.1128/EC.00149-14

maintenance of carbon dioxide tension. The method is suitable for application to both PS and BS cells, as they remain in a viable state for an extended time period. Furthermore, this technique facilitates FRAP, as shown by the full fluorescence recovery of photobleached mitochondrion-targeted yellow fluorescent protein (MT-YFP), indicating the healthy physical state of cells immobilized by our technique.

Establishing this platform for imaging of live *T. b. brucei* has allowed us to analyze the dynamics of the mitochondrial RNA-binding protein 1 and 2 (MRP1/2) complex in the nanostructured compartment of the mitochondrial matrix. This abundant complex is a heterotetramer consisting of two each of the MRP1 (TriTrypDB accession no. Tb927.11.1710) and MRP2 (accession no. Tb927.11.13280) subunits (14, 15). Although these two proteins have low sequence identity, they remarkably share a tertiary structure that forms a “Whirly” transcription factor fold. The tetramerization of MRP1 and -2 creates an electropositive face that allows the complex’s nonspecific interaction with the negatively charged phosphate groups of the RNA backbone. This mode of binding exposes the bases of each nucleotide outward, which would be amenable to a suggested role for the MRP1/2 complex as an RNA matchmaker, which facilitates annealing of gRNA and mRNA molecules (14–17). However, functional analysis of MRP1/2 has suggested that this complex may play a wider role in mitochondrial RNA metabolism in addition to or instead of RNA editing (18–20).

Here we address for the first time mitochondrial RNA metabolism in live trypanosomes by studying the motility and dynamics of MRP1 under two strikingly different conditions. We contrast the *T. b. brucei* BS, which has an intact kDNA encoding transcripts that are duly processed by the elaborate pathway residing in the mitochondrion, with *T. b. evansi*. The mitochondrion of this kinetoplastic (AK) subspecies is devoid of any organellar DNA or RNA. Thus, these trypanosomes can be considered an analog to rho<sup>0</sup> petite mutant *Saccharomyces cerevisiae*, which also lacks mitochondrial DNA (9, 21, 22). Yet, AK *T. b. evansi* still imports the protein machinery required for RNA processing despite the lack of substrate nucleic acids, as well as all tRNAs (21, 23–25). Among the imported macromolecular complexes assembled from the imported proteins are the MRP1/2 heterotetramer and a catalytically active RNA-editing core complex (RECC) that coordinates the enzymatic steps required for U insertion/deletion (21, 25). Indeed, C-terminally tagged MRP1, serving as a proxy for the whole complex, exhibits less translational diffusion within the BS mitochondrion than in AK *T. b. evansi*, which can be explained by the lack of mitochondrion-encoded nucleic acids in the latter compartment. These results provide a novel insight into the environment of the organelle and may be applicable to the study of other mitochondrial proteins.

## MATERIALS AND METHODS

**Generation of cell lines.** Lister 427 strains of PS and BS *T. b. brucei* and Antat 3/3 *T. b. evansi* were cultured, transfected, and screened for the appropriate drug resistance of a given construct as described previously (9, 26). The construct pMT-YFP, modified from the pDEX557-Y plasmid (27) to include the mitochondrial signal peptide from the *Naegleria gruberi* iron dehydrogenase gene between the HindIII and XhoI restriction sites upstream of the YFP gene, was employed to generate MT-YFP cell lines. For *in situ* C-terminal tagging of MRP1 with YFP, the full ORF excluding the stop codon was PCR amplified with forward primer 5′-TAGGGCGAATTGGATGATTCGACTCGCATGCCTGCGT-3′ and re-

verse primer 5′-ACCATTCCGCCACCGGAATGGTATCGCGATGTGTCACTTAC-3′. The PCR amplicon was cloned into the p2937 vector (27) via the homology flanks introduced into the PCR primers (underlined) with the GeneArt Seamless Cloning kit according to the manufacturer’s (Invitrogen) protocol.

**Confocal microscopy.** In order to visualize mitochondria,  $5 \times 10^6$  to  $1 \times 10^7$  PS *T. brucei* cells were incubated in semidefined medium 79 (SDM-79) supplemented with 200 nM MitoTracker Red CMXRos (Molecular Probes) for 20 min at 27°C, while  $5 \times 10^6$  to  $1 \times 10^7$  BS *T. brucei* cells were incubated in Hirumi’s modified Iscove’s medium 9 (HMI-9) with 20 nM MitoTracker Red for 20 min at 37°C. Cells were subsequently immobilized by the method described below. They were examined on an Olympus FluoView FV1000 confocal microscope with the accompanying FluoView v1.7 software and a 488-nm laser for YFP scanning and a 559-nm laser for the propidium iodide (PI) and Mitotracker Red CMXRos dyes, respectively. All images were processed and collected with a 100× oil immersion objective at 25°C. Line scanning of the merged images was done by drawing a test line across the cell intersecting the mitochondrion and measuring the relative fluorescence intensity along the line with the ImageJ software (28).

**Trypanosome immobilization.** Research grade agarose (Serva) was dissolved in heated phosphate-buffered saline (PBS) supplemented with 6 mM D-glucose (PDSG) to a concentration of 1% (wt/vol). A 12-ml volume was poured into a 9.2-cm-diameter petri dish (SPL) and left to solidify, which ensures a sheet of agarose with a thickness of about 2 mm. The agarose block can be prepared in advance and stored for 1 month sealed at 4°C until use. In the meantime, PS, BS, and *T. b. evansi* cells were centrifuged at  $900 \times g$  for 2 min and washed once with prewarmed PDSG (25°C for PS cells and 37°C for BS and AK *T. b. evansi* cells) under the same centrifugation conditions. The cells were gently suspended in 200  $\mu$ l of phenol red-free Iscove’s modified Dulbecco’s medium (IMDM; Invitrogen) prewarmed to the appropriate temperature based on a given cell stage. Five microliters was dropped onto a 24-by-60-mm coverslip (Prestige), which was immediately and gently covered with a 1-by-1-cm agarose block cut from the petri dish. The coverslip was fixed onto an inverted Olympus FluoView FV1000 confocal microscope on top of two microscope slides with Plasticine (see Fig. 1A; also see Fig. S1 in the supplemental material). Cells were kept at the appropriate temperature with a heat block before immobilization.

**FRAP analysis.** Cells that were immobilized for up to 30 min were used in FRAP experiments. A series of 250 images (800 by 800 pixels, 10  $\mu$ s/pixel; frame time, 0.336 s) were acquired with a 170- $\mu$ m pinhole and sequential multitrack imaging with a 488-nm laser (5% transmission for acquisition). The simultaneous-scanning SIM Scanner system was used with a 405-nm laser whose intensity was adjusted for 50 to 75% photobleaching in a circular region of interest (ROI) with a diameter of 0.35  $\mu$ m. Per replicate, an individual cell was bleached only once. The average fluorescence intensity  $F(t)$  within the bleached region was calculated with the FRAP accessory tool in the FluoView v1.7 program (Olympus). The  $F(t)$  in the background and in the unbleached region of the same cell were measured to normalize FRAP recovery curves by using the following equation (28, 29):  $F(t)_{\text{norm}} = [F(t)_{\text{ROI}} - F(t)_{\text{bkgd}}](F_{i,\text{non}} - F_{i,\text{bkgd}})/[F(t)_{\text{non}} - F(t)_{\text{bkgd}}](F_{i,\text{ROI}} - F_{i,\text{bkgd}})$ .

The bleached ROI intensity  $[F(t)_{\text{ROI}}]$  and the nonbleached region intensity  $[F(t)_{\text{non}}]$  are corrected with the background intensity  $[F(t)_{\text{bkgd}}]$  at each time point ( $t$ ) and divided by the corrected intensity of the nonbleached region for the loss of fluorescence during the time course of the experiment. Next, the data are normalized to the background-corrected prebleach intensity ( $F_i$ ) in the nonbleached region, the background region, and the ROI ( $F_{i,\text{non}}$ ,  $F_{i,\text{bkgd}}$ , and  $F_{i,\text{ROI}}$ , respectively). By using the first time point after the bleach set as  $t = 0$ , the fluorescence intensity recovery ratio  $[F(t)_R]$  at each time point can be calculated to generate mean recovery curves (see Fig. 2D to F and 3E to F) by using the mean value of every five sequential scanning measurements as follows:  $F(t)_R = [F(t)_{\text{norm}} - F(0)]/[1 - F(0)]$ .

In order to obtain the  $T_{50\%}$  and  $R_{\max}$  values, which indicate the translational diffusion and motile fraction of the photobleached fluorescent protein, the FRAP recovery curve from each replicate per sample was fitted by the single-component exponential model in the equation  $F(t) = A(1 - e^{-t/TFRAP})$  (29).

$T_{50\%}$  was calculated from the fitted-curve model for each FRAP experiment. The mobile fraction was equal to  $R_{\max}$ , the maximal recovery of fluorescence compared to the prebleach values from this equation when  $t = \infty$  (29–31). The values obtained from each FRAP experiment, see Tables S1 to S6 in the supplemental material, and the means and standard deviations (SDs) of these values are shown below the FRAP images in Fig. 2D to F and 3E to F. The statistical significance of the difference between the MRP1-YFP  $R_{\max}$  values of BS and AK *T. b. evansi* was calculated by unpaired Student *t* test by using the determined mean  $R_{\max}$ , SD, and number of replicates (*n*).

**Immunoprecipitation and Western blot analysis.** Immunoprecipitation was carried out with  $1 \times 10^8$  BS and *T. b. evansi* protozoa expressing MRP1-YFP. Lysates from these cells were incubated with anti-green-fluorescent-protein (anti-GFP) monoclonal antibody 3E6 (Molecular Probes) bound to Dynabeads protein G (Invitrogen) for 12 h at 4°C in the presence of Complete protease inhibitor according to the manufacturer's (Roche) recommendation. The flowthrough fraction was collected for subsequent Western blot analysis, and the column was washed three times with 200  $\mu$ l of PBS with 0.05% Tween 40. The antibody-antigen interaction was disrupted by elution three times with 50  $\mu$ l of 100 mM glycine (pH 2.5), and the eluates were neutralized with 1 M Tris buffer (pH 8.7) and analyzed by Western blotting as previously described (26).

## RESULTS

### Viability of PS and BS trypanosomes under immobilizing conditions.

Cells constitutively expressing MT-YFP were gently centrifuged, and after the growth medium was discarded, they were resuspended in IMDM. In addition to lacking the phenol red present in the growth medium for BS and PS *in vitro* cultures, which can interfere with fluorescence assays, IMDM contains D-glucose and HEPES, a buffer that maintains a physiological pH despite changes in the concentration of carbon dioxide (32). A drop of the cell suspension was applied to a coverslip fixed onto an inverted confocal microscope (Fig. 1A; see Fig. S1 in the supplemental material). This drop was immediately covered with a thin layer of agarose to restrain the cells and also mitigate cell desiccation.

The viability of immobilized *T. b. brucei* was first determined by staining with PI added to IMDM. Because of selective penetration of the compound into dead cells, the number of viable cells was determined by counting PI staining-negative cells. Initially, about 99% of the PS and BS protozoa were fully viable, reflecting the mild harvesting and immobilizing process (Fig. 1B and C). Within 3 h under the immobilization condition at room temperature, the percentage of viable PS cells remained above 90%, with the surviving cells exhibiting normal morphology and a homogeneous distribution of MT-YFP, a reflection of the vitality of the organelle. Viability dropped to 80 and 60% after 4 and 6 h, respectively. At this final time point, dead cells exhibited a swollen morphology and the MT-YFP showed a fragmented distribution, representing the disintegration of mitochondria.

For BS, the percentage of viable cells remained above 90% for the first 2 h of immobilization, with MT-YFP evenly distributed throughout the organelle (Fig. 1D). Hence, this time frame can be recommended for live-cell imaging experiments. After 3 h, viability under these conditions declined sharply, with the overall appearance of swollen cell morphology and mitochondrial fragmentation. Under our established immobilization conditions, viable

cells at both stages exhibited limited membrane and/or flagellar undulation, although they were fixed in place (see Movies S1 and S2 in the supplemental material). Furthermore, the procedure developed promotes a population of consistently immobilized and evenly distributed cells.

### Trypanosome immobilization facilitates FRAP experiments.

Although the viability assays showed that the absolute majority of both PS and BS cells was healthy and viable for at least 2 h, the potential effect of immobilization on mitochondrial physiology remained unknown. Therefore, we decided first to test whether our immobilization protocol allows the application of FRAP to the mitochondrion, which is the organelle of interest to us. Using the results of the previous experiments as a guideline, we performed immobilization within 30 min in all subsequent experiments.

We started with the measurement of the translational diffusion of YFP, equipped with the mitochondrial import signal from *N. gruberi* iron hydrogenase (MT-YFP) (33), in immobilized PS and BS plus AK *T. b. evansi* cells. In all cases, MT-YFP exhibited consistent colocalization with the Mitotracker Red dye, indicating an even distribution of the tagged protein within the mitochondrion (Fig. 2A to C). On the basis of this, the photobleaching spots for the FRAP analysis were randomly selected in the mitochondrial compartment of an individual cell. In PS cells, MT-YFP reached 50% recovery ( $T_{50\%}$ ) of the prebleaching fluorescence intensity within the bleached ROI at  $4.44 \pm 2.82$  s after bleaching (Fig. 2D), as well as achieving full recovery of fluorescence over the time course ( $R_{\max} = 1.02 \pm 0.128$ ), indicating that diffusion of YFP is unhindered in the matrix.

In BS and AK *T. b. evansi* cells, the YFP recovery profiles in the ROI appeared to be almost identical, with  $T_{50\%}$  values of  $2.96 \pm 2.30$  and  $3.44 \pm 1.67$  s, respectively, and virtually full recovery of prebleaching fluorescence intensity ( $R_{\max} = 0.97 \pm 0.169$  and  $0.94 \pm 0.165$ , respectively) (Fig. 2E and F). In summary, these data show that our immobilization method is appropriate for FRAP analysis of BS and PS, as well as AK *T. b. evansi*, cells. The recovery of MT-YFP fluorescence in these immobilized trypanosomes is also indicative of their viable condition, as no such recovery was detected in the photobleached ROIs of PS cells exhibiting a fragmented mitochondrial morphology (see Fig. S2 in the supplemental material), which also stained with the dead-cell marker PI (Fig. 1D). Moreover, since a substantial fraction of YFP remained in a diffused state and recovered rapidly after bleaching, this protein qualifies as a suitable fluorescent tag for tracking the mobility of other mitochondrial proteins in *T. brucei*.

### The MRP1/2 complex exhibits different dynamics in *T. b. brucei* and AK *T. b. evansi*.

In order to investigate the dynamics of the MRP1/2 complex, we generated both BS and AK *T. b. evansi* cell lines carrying *in situ* C-terminally YFP-tagged MRP1 (MRP1-YFP). Because the latter cell type is locked in the slender pathogenic stage (9, 21), only BS *T. b. brucei* was used in the comparative FRAP analysis, which capitalized on the dramatic difference between these cell lines in terms of the absence or presence of nucleic acids in their respective organelles.

First, we compared the abundance of MRP1-YFP in BS and AK protozoa by immunodecoration of Western blot assays of respective whole-cell lysates with anti-GFP antibody, which showed no differences in expression between the two cell lines (Fig. 3A). Next, to confirm that YFP tagging does not interfere with the incorporation of MRP1 into the MRP1/2 complex *in vivo*, we immunoprecipitated tagged MRP1 with an anti-GFP

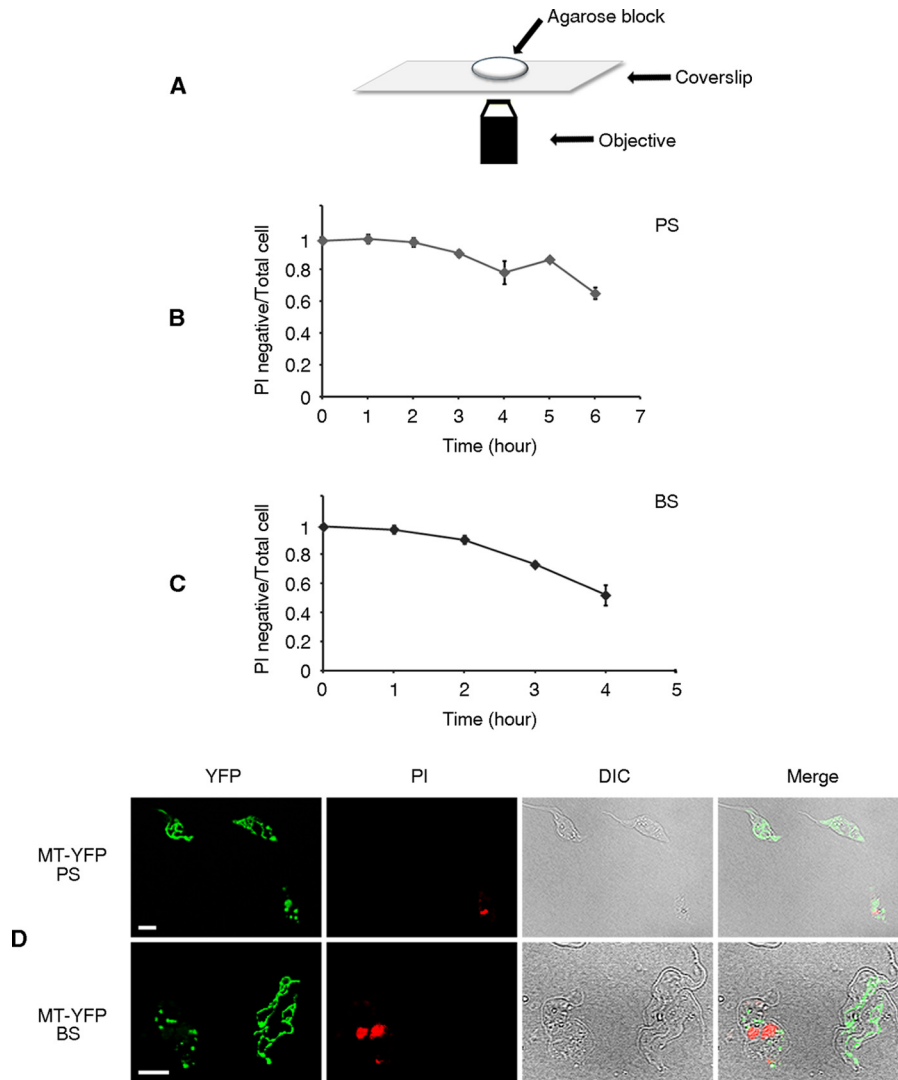


**FIG 1** Parasite viability under agarose block immobilization conditions. (A) Schematic depicting the apparatus used to monitor trypanosomes immobilized with a 1% agarose block with an inverted microscope. (B) *T. b. brucei* PS viability was determined following immobilization as depicted in panel A. Harvested trypanosomes were resuspended gently in IMDM containing 5  $\mu\text{g/ml}$  PI. PI exclusion was used as a marker of viability, and cell viability is plotted on the y axis as PI-negative cells/total cells. More than 200 cells were counted per time point in triplicate. (C) BS *T. b. brucei* viability was determined as described for panel B. (D) Representative imagines of PS and BS trypanosomes immobilized for 1 h. Scale bars, 10  $\mu\text{m}$ .

antibody (Fig. 3B) and looked for the presence of endogenous MRP1 and MRP2 with antibodies against each of these subunits (20). Since C-terminally tagged MRP1 coimmunoprecipitated with the endogenous subunits in both BS *T. b. brucei* and AK *T. b. evansi*, MRP1-YFP is properly assembled into the MRP1/2 complex. The band intensities of the MRP1-YFP versus the endogenous MRP1 suggest that the stoichiometry of the former ranges from two to one copies. Thus, the subsequent FRAP experiment is relevant for the MRP1/2 complex as a whole. Furthermore, coimmunoprecipitation of the intact MRP1/2 complex in AK *T. b. evansi* (Fig. 3B) indicates that the complex is properly assembled even in the absence of RNA. The MRP1-YFP protein consistently colocalized with the Mitotracker Red signal, proving that there is an even distribution of the tagged protein in the mitochondrial lumen of both cell lines

and that this localization pattern is independent of the presence or absence of organelle-encoded RNA (Fig. 3C and D).

The photobleached ROIs for FRAP were selected randomly as in the case of MT-YFP. Hence, the results reflect the general profile of MRP1 throughout the organelle. In the FRAP analysis, MRP1-YFP did not show full recovery in BS *T. b. brucei* or in AK *T. b. evansi*. The mobile fraction of the YFP-tagged protein, as reflected in the  $R_{\text{max}}$  value in the BS ROI, was  $0.47 \pm 0.188$  (Fig. 3E), while that of AK *T. b. evansi* was  $0.71 \pm 0.175$  (Fig. 3F). This difference between the mean  $R_{\text{max}}$  values obtained from fitted curves from all of the replicates of each sample is statistically significant ( $P = 0.001$ ). The MRP1/2 complex thus exhibits significantly higher motility in the mitochondrial lumen of *T. b. evansi*, which differs from the BS by the absence of organellar RNA. Furthermore, the presence of an immobile fraction, as demonstrated by the *T. b.*

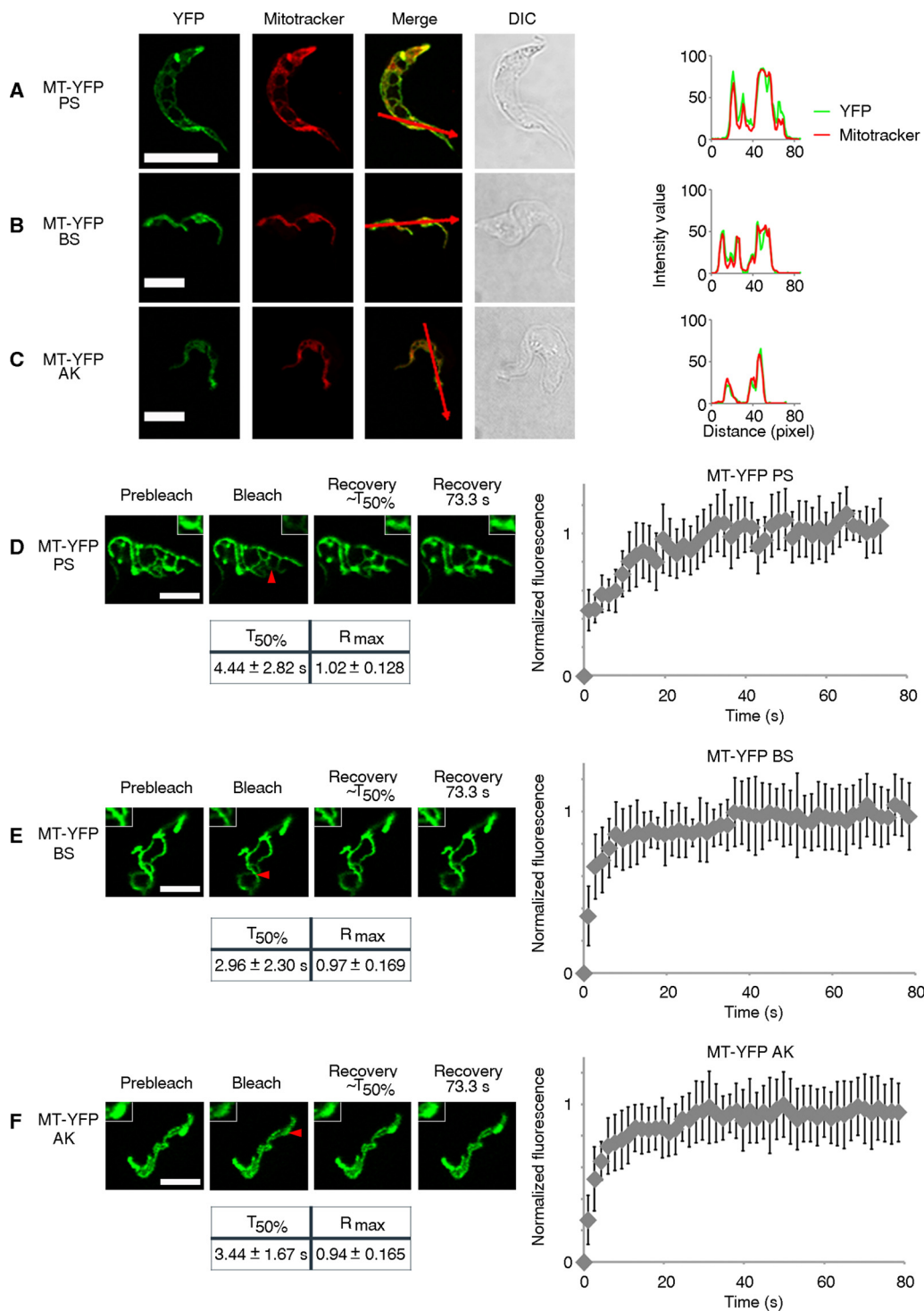


**FIG 2** FRAP analysis of mitochondrion-targeted YFP in live immobilized trypanosomes. (A to C) Mitochondrial localization and distribution of MT-YFP in PS *T. b. brucei* (A), BS *T. b. brucei* (B), and AK *T. b. evansi* (C). From left to right, the YFP and Mitotracker Red channels are indicated at the top, followed by a merged view of both images in which the trace of the line scan used to measure each channel's fluorescence intensity is indicated by a red arrow. The plotted intensities along the line are shown to the right of the differential interference contrast (DIC) images of the trypanosomes. (D to F) FRAP analysis of MT-YFP in PS *T. b. brucei* (D), BS *T. b. brucei* (E), and AK *T. b. evansi* (F). To the left are representative images acquired in a FRAP experiment during, from left to right, the prebleaching, bleached, and approximate  $T_{50\%}$  and maximal-recovery time points. The photobleached ROI is indicated by the red arrowhead in the bleached image and is enlarged  $\times 2.5$  in the insets. To the right are the average fluorescence recovery curves from PS ( $n = 14$  cells) plus BS and AK ( $n = 15$  cells) trypanosomes, normalized as described in Materials and Methods. The mean  $T_{50\%}$  and  $R_{max}$  values  $\pm$  SDs determined from the fitted curves generated from these measurements (for data obtained from the fitted curves for each replicate of PS, BS, and AK trypanosomes, see Tables S1 to S3 in the supplemental material) are shown below the FRAP images. Scale bars, 10  $\mu$ m (A) and 5  $\mu$ m (B to F).



## DISCUSSION

The development of live-imaging techniques such as FRAP and FCS has been instrumental in advancing our knowledge of cell biology, such as addressing spliceosome assembly in HeLa cells (28, 34). In contrast to the situation in adherent cell types, the use of these techniques in *T. brucei* and related flagellates has been hampered by their highly motile nature, which is an essential part of their biology (7, 12). In this work, we describe an immobilization method that overcomes this problem and opens an opportunity to exploit the simple architecture of trypanosomes for this line of research (1). The method is rapid, economical, and reproducible, using a thin agarose block to restrain cells on top of a coverslip for visualization with an inverted microscope. The gentle preparation protocol, which avoids the brief drying steps of other immobilization protocols (2, 8), is robust enough for application to both PS and BS *in vitro* cultures, which are life stages with very different physiological states (5).

An essential prerequisite for such studies is that the cells be maintained in a vital state. In order to validate the method, we assayed the viability of trypanosomes by scoring for the percentage of dead cells that incorporate PI in the two life cycle stages tested. According to this assay, cell viability is maintained for 3 h for the PS and 2 h for the BS. These results were confirmed by the morphology of the mitochondrion, which eventually took on a fragmented appearance as cells began to regress, as visualized by leader sequence-directed MT-YFP.

The MT-YFP-expressing cell lines were further investigated by FRAP in order to better assess the condition of the trypanosomes, as well as test the suitability of this type of immobilization for such live-imaging techniques. In contrast to the situation with cytosolic GFP-expressing *L. major* embedded in a CyGEL matrix (12), the photobleached ROI exhibited full recovery in PS, BS, and AK MT-YFP trypanosomes. This observation is consistent with a healthy state of the immobilized flagellates, as it reproduces robust recovery results from FRAP with mitochondrion-targeted GFP in adherent mammalian cell lines (29, 35), a system that does not require immobilization steps that could affect cell viability. Furthermore, no such recovery was seen in dying trypanosomes upon FRAP of MT-YFP. The immobilization technique also proved to restrain cells in a manner suitable for recording of fluorescence recovery within an approximately 0.1- $\mu\text{m}^2$  ROI.

With the utility of FRAP on trypanosomes immobilized by our new technique confirmed, we decided to investigate the dynamics of the *in situ* C-terminally tagged MRP1-YFP, which was verified to be incorporated into the abundant RNA-binding MRP1/2 complex (14, 15, 17). The dynamics of the MRP1/2 complex were compared in BS and AK *T. b. evansi* cells to determine the influence of mitochondrion-encoded RNAs, which are absent from the latter subspecies (9, 21, 23). In the BS, more of the MRP1/2 complex was in an immobile fraction than in AK *T. b. evansi*, as it achieved an  $R_{\text{max}}$  of  $0.47 \pm 0.188$  of the prebleach fluorescence within the photobleached ROI compared to an  $R_{\text{max}}$  of  $0.71 \pm 0.175$  in AK cells. The presence of mitochondrion-encoded RNA clearly hinders the dynamics of the MRP1/2 complex (Fig. 4A). We exclude the possibility that physiological changes in the AK mitochondrion that are due to the mitochondrion-encoded subunit of  $F_0F_1$ -ATP synthase and compensatory mutations in the nucleus-encoded  $\gamma$  subunit (9, 22) underlie this difference in the translational diffusion of MRP1/2 because MT-YFP

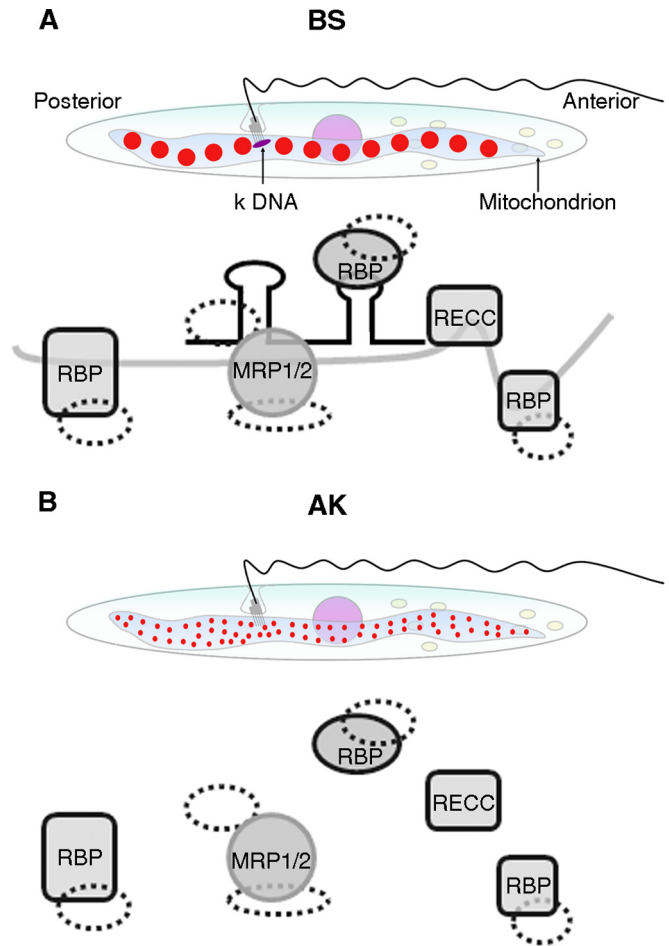


FIG 4 Schematic illustration of RNA-processing protein complexes in BS and AK trypanosomes. (A) RNA-protein complex distribution in the BS. In the presence of kDNA and its encoded RNA, MRP1/2 exists in RNA-protein complexes (large red circles), which are evenly distributed throughout the whole mitochondrial matrix and associated with other proteins coating the same RNA. The gray schemes below the cell models show that MRP1/2-bound RNA is undergoing the RNA-editing process with the RECC, gRNA, and other RNA-binding proteins (RBP) bound to the same RNA molecule. The dashed circles represent speculated proteins bound directly to MRP1/2 and other proteins. (B) Distribution and construction of the RNA-processing protein complex with the absence of RNA in AK *T. b. evansi*. In the absence of kDNA and organelle-encoded RNA, identical proteins involved in RNA processing shown in panel A are still scattered throughout the mitochondrial matrix but as smaller complexes not aggregating around RNA (small red circles). The gray scheme below the cell model shows that MRP1/2 is perhaps bound to other proteins, depicted as dashed circles as in panel A. Other proteins that interact with MRP1/2 via RNA linkers in panel A are shown but are independent of MRP1/2 in AK *T. b. evansi*.

exhibits similar dynamics within the matrix compartment of both types of organelles. Other proteins simultaneously coating RNAs bound to MRP1/2 may contribute to this apparent drag in BS, as the MRP1/2 complex has been shown in the related trypanosomatid *Leishmania tarentolae* to associate via RNA with the RECC, conferring the core enzymatic activities needed for RNA editing, and members of mitochondrial RNA-binding complex 1 (17), which plays an ancillary role in the process (36).

Surprisingly, the MRP1/2 complex in AK *T. b. evansi* does not fully recover to prephotobleached levels within the MRP1-YFP1

ROI. Even in this environment without mitochondrion-encoded RNA, there is an immobile fraction of the heterotetramer. There are some possible explanations for this phenomenon (Fig. 4B). The first one postulates that the MRP1/2 complex interacts with other proteins in an RNA-independent manner. However, there is very little evidence thus far that the MRP1/2 complex interacts with any polypeptides outside the complex (37). Alternatively, the MRP1/2 complex may interact with tRNAs that are futilely imported into the AK mitochondrion, although proteins that normally bind these nucleic acids to facilitate their role in translation are also present (23, 24), likely sequestering them from spurious interaction with MRP1/2. Another possibility is that the 125- to 150-kDa MRP1/2 complex, bearing one or two copies of MRP1-YFP, is more prone to molecular sieving effects within the matrix than MT-YFP is, leading to an apparent immobile fraction. Finally, association with another structure within the mitochondrion, such as the inner membrane, may hinder a fraction of MRP1/2. Mitochondrial RNA metabolism pathways could be located in proximity to the inner membrane, where translation of mature mRNAs by mitochondrial ribosomes occurs to facilitate the incorporation of nascent polypeptides into the lipid bilayer (38). MRP1/2 association with this part of the organelle in the AK trypanosome could be a vestige of this now obsolete process.

The translational diffusion of the MRP1/2 complex was also assayed in PS *T. b. brucei*. While an immobile fraction of the complex was observed, it was much smaller than that in the BS. However, direct comparison of these results between the BS and the PS is more complicated than that made between BS and AK *T. b. evansi*. For instance, the two life cycle stages harbor mitochondria that have very different morphological and physiological states, which could have differing impacts on the translational diffusion of the matrix proteins. Furthermore, the mitochondrial transcriptomes differ between the PS and the slender BS by a still unknown mechanism and extent (39). Perhaps this observation may be due in part to this phenomenon.

The immobilization technique developed for this study has allowed us to exploit the availability of AK *T. b. evansi* *in vitro* cultures to study the impact of RNA on the dynamics of the abundant RNA-binding MRP1/2 complex. Until now, the behaviors of proteins involved in mitochondrial RNA metabolism have not been explored in live cells. The use of FRAP has brought a different perspective not only to our current knowledge about the MRP1/2 tetramer but also to how RNA can affect the dynamics of proteins involved in the byzantine RNA metabolism of the trypanosome mitochondrion, in which hundreds of proteins in several complexes are coordinated to express the few proteins encoded by kDNA.

## ACKNOWLEDGMENTS

We thank Michael Ginger (University of Lancaster, Lancaster, United Kingdom) and Mark Carrington (University of Cambridge, Cambridge, United Kingdom) for pDEX577-Y and p2937 and Achim Schnauffer (University of Edinburgh, Edinburgh, United Kingdom) for providing the *T. b. evansi* cell line. We thank Martin Hof and Jan Sýkora (J. Heyrovský Institute of Physical Chemistry, Czech Republic), as well as Maria Carmo-Fonseca and José Rino (Instituto de Medicina Molecular, Portugal) and Radek Kaňa (Institute of Microbiology, Czech Republic), for enlightening discussions and valuable advice.

This work was supported by the Czech grant agency (P305/12/2261), the RNPnet FP7 program (289007), Bioglobe grant CZ.1.07/2.3.00/30.0032, and a Praemium Academiae award to J.L., who is also a Fellow of

the Canadian Institute for Advanced Research. We acknowledge the use of research infrastructure funded from EU 7th Framework program 316304.

## REFERENCES

- Matthews KR. 2005. The developmental cell biology of *Trypanosoma brucei*. *J. Cell Sci.* 118:283–290. <http://dx.doi.org/10.1242/jcs.01649>.
- Ho HH, He CY, de Graffenried CL, Murrells LJ, Warren G. 2006. Ordered assembly of the duplicating Golgi in *Trypanosoma brucei*. *Proc. Natl. Acad. Sci. U. S. A.* 103:7676–7681. <http://dx.doi.org/10.1073/pnas.0602595103>.
- He CY, Pypaert M, Warren G. 2005. Golgi duplication in *Trypanosoma brucei* requires Centrin2. *Science* 310:1196–1198. <http://dx.doi.org/10.1126/science.1119969>.
- Lukeš J, Hashimi H, Verner Z, Čičová Z. 2010. The remarkable mitochondrion of trypanosomes and related flagellates, p 227–252. *In de Souza W (ed), Structures and organelles in pathogenic protists.* Springer, Berlin, Germany.
- Bringaud F, Riviere L, Coustou V. 2006. Energy metabolism of trypanosomatids: adaptation to available carbon sources. *Mol. Biochem. Parasitol.* 149:1–9. <http://dx.doi.org/10.1016/j.molbiopara.2006.03.017>.
- Gordon GW, Berry G, Liang XH, Levine B, Herman B. 1998. Quantitative fluorescence resonance energy transfer measurements using fluorescence microscopy. *Biophys. J.* 74:2702–2713. [http://dx.doi.org/10.1016/S0006-3495\(98\)77976-7](http://dx.doi.org/10.1016/S0006-3495(98)77976-7).
- Broadhead R, Dawe HR, Farr H, Griffiths S, Hart SR, Portman N, Shaw MK, Ginger ML, Gaskell SJ, McKean PG, Gull K. 2006. Flagellar motility is required for the viability of the bloodstream trypanosome. *Nature* 440:224–227. <http://dx.doi.org/10.1038/nature04541>.
- Pérez-Morga D, Vanhollebeke B, Paturiaux-Hanocq F, Nolan DP, Lins L, Hombler F, Vanhamme L, Tebabi P, Pays A, Poelvoorde P, Jaquet A, Brasseur R, Pays E. 2005. Apolipoprotein L-I promotes trypanosome lysis by forming pores in lysosomal membranes. *Science* 309:469–472. <http://dx.doi.org/10.1126/science.1114566>.
- Schnauffer A, Clark-Walker GD, Steinberg AG, Stuart K. 2005. The F1-ATP synthase complex in bloodstream stage trypanosomes has an unusual and essential function. *EMBO J.* 24:4029–4040. <http://dx.doi.org/10.1038/sj.emboj.7600862>.
- Esson HJ, Morriswood B, Yavuz S, Vidilaseris K, Dong G, Warren G. 2012. Morphology of the trypanosome bilobe, a novel cytoskeletal structure. *Eukaryot. Cell* 11:761–772. <http://dx.doi.org/10.1128/EC.05287-11>.
- Buisson J, Chenouard N, Lagache T, Blisnick T, Olivo-Marin JC, Bastin P. 2013. Intraflagellar transport proteins cycle between the flagellum and its base. *J. Cell Sci.* 126:327–338. <http://dx.doi.org/10.1242/jcs.117069>.
- Price HP, MacLean L, Marrison J, O'Toole PJ, Smith DF. 2010. Validation of a new method for immobilising kinetoplastid parasites for live cell imaging. *Mol. Biochem. Parasitol.* 169:66–69. <http://dx.doi.org/10.1016/j.molbiopara.2009.09.008>.
- Maclean LM, O'Toole PJ, Stark M, Marrison J, Seelenmeyer C, Nickel W, Smith DF. 2012. Trafficking and release of *Leishmania* metacyclic HASPB on macrophage invasion. *Cell. Microbiol.* 14:740–761. <http://dx.doi.org/10.1111/j.1462-5822.2012.01756.x>.
- Zíková A, Kopečná J, Schumacher MA, Stuart K, Trantírek L, Lukeš J. 2008. Structure and function of the native and recombinant mitochondrial MRP1/MRP2 complex from *Trypanosoma brucei*. *Int. J. Parasitol.* 38:901–912. <http://dx.doi.org/10.1016/j.ijpara.2007.12.009>.
- Schumacher MA, Karamooz E, Zíková A, Trantírek L, Lukeš J. 2006. Crystal structures of *T. brucei* MRP1/MRP2 guide-RNA binding complex reveal RNA matchmaking mechanism. *Cell* 126:701–711. <http://dx.doi.org/10.1016/j.cell.2006.06.047>.
- Müller UF, Lambert L, Goring HU. 2001. Annealing of RNA editing substrates facilitated by guide RNA-binding protein gBP21. *EMBO J.* 20:1394–1404. <http://dx.doi.org/10.1093/emboj/20.6.1394>.
- Aphasizhev R, Aphasizheva I, Nelson RE, Simpson L. 2003. A 100-kD complex of two RNA-binding proteins from mitochondria of *Leishmania tarentolae* catalyzes RNA annealing and interacts with several RNA editing components. *RNA* 9:62–76. <http://dx.doi.org/10.1261/rna.2134303>.
- Fisk JC, Presnyak V, Ammerman ML, Read LK. 2009. Distinct and overlapping functions of MRP1/2 and RBP16 in mitochondrial RNA metabolism. *Mol. Cell. Biol.* 29:5214–5225. <http://dx.doi.org/10.1128/MCB.00520-09>.
- Lambert L, Müller UF, Souza AE, Goring HU. 1999. The involvement of gRNA-binding protein gBP21 in RNA editing—an *in vitro* and *in vivo*

- analysis. *Nucleic Acids Res.* 27:1429–1436. <http://dx.doi.org/10.1093/nar/27.6.1429>.
20. Vondrusková E, van den Burg J, Zíková A, Ernst NL, Stuart K, Benne R, Lukeš J. 2005. RNA interference analyses suggest a transcript-specific regulatory role for mitochondrial RNA-binding proteins MRP1 and MRP2 in RNA editing and other RNA processing in *Trypanosoma brucei*. *J. Biol. Chem.* 280:2429–2438. <http://dx.doi.org/10.1074/jbc.M405933200>.
  21. Lai DH, Hashimi H, Lun ZR, Ayala FJ, Lukeš J. 2008. Adaptations of *Trypanosoma brucei* to gradual loss of kinetoplast DNA: *Trypanosoma equiperdum* and *Trypanosoma evansi* are petite mutants of *T. brucei*. *Proc. Natl. Acad. Sci. U. S. A.* 105:1999–2004. <http://dx.doi.org/10.1073/pnas.0711799105>.
  22. Dean S, Gould MK, Dewar CE, Schnauffer AC. 2013. Single point mutations in ATP synthase compensate for mitochondrial genome loss in trypanosomes. *Proc. Natl. Acad. Sci. U. S. A.* 110:14741–14746. <http://dx.doi.org/10.1073/pnas.1305404110>.
  23. Paris Z, Hashimi H, Lun S, Alfonso JD, Lukeš J. 2011. Futile import of tRNAs and proteins into the mitochondrion of *Trypanosoma brucei evansi*. *Mol. Biochem. Parasitol.* 176:116–120. <http://dx.doi.org/10.1016/j.molbiopara.2010.12.010>.
  24. Cristodero M, Seebeck T, Schneider A. 2010. Mitochondrial translation is essential in bloodstream forms of *Trypanosoma brucei*. *Mol. Microbiol.* 78:757–769. <http://dx.doi.org/10.1111/j.1365-2958.2010.07368.x>.
  25. Domingo GJ, Palazzo SS, Wang B, Pannicucci B, Salavati R, Stuart KD. 2003. Dyskinetoplastic *Trypanosoma brucei* contains functional editing complexes. *Eukaryot. Cell* 2:569–577. <http://dx.doi.org/10.1128/EC.2.3.569-577.2003>.
  26. Hashimi H, McDonald I, Stríbrná E, Lukeš J. 2013. Trypanosome Letm1 protein is essential for mitochondrial potassium homeostasis. *J. Biol. Chem.* 288:26914–26925. <http://dx.doi.org/10.1074/jbc.M113.495119>.
  27. Kelly S, Reed J, Kramer S, Ellis L, Webb H, Sunter J, Salje J, Marinsek N, Gull K, Wickstead B, Carrington M. 2007. Functional genomics in *Trypanosoma brucei*: a collection of vectors for the expression of tagged proteins from endogenous and ectopic gene loci. *Mol. Biochem. Parasitol.* 154:103–109. <http://dx.doi.org/10.1016/j.molbiopara.2007.03.012>.
  28. Martins SB, Rino J, Carvalho T, Carvalho C, Yoshida M, Klose JM, de Almeida SF, Carmo-Fonseca M. 2011. Spliceosome assembly is coupled to RNA polymerase II dynamics at the 3' end of human genes. *Nat. Struct. Mol. Biol.* 18:1115–1123. <http://dx.doi.org/10.1038/nsmb.2124>.
  29. Dieteren CE, Gielen SC, Nijtmans LG, Smeitink JA, Swarts HG, Brock R, Willems PH, Koopman WJ. 2011. Solute diffusion is hindered in the mitochondrial matrix. *Proc. Natl. Acad. Sci. U. S. A.* 108:8657–8662. <http://dx.doi.org/10.1073/pnas.1017581108>.
  30. Kaňa R. 2013. Mobility of photosynthetic proteins. *Photosynth. Res.* 116:465–479. <http://dx.doi.org/10.1007/s11120-013-9898-y>.
  31. Goodwin JS, Kenworthy AK. 2005. Photobleaching approaches to investigate diffusional mobility and trafficking of Ras in living cells. *Methods* 37:154–164. <http://dx.doi.org/10.1016/j.ymeth.2005.05.013>.
  32. Baicu SC, Taylor MJ. 2002. Acid-base buffering in organ preservation solutions as a function of temperature: new parameters for comparing buffer capacity and efficiency. *Cryobiology* 45:33–48. [http://dx.doi.org/10.1016/S0011-2240\(02\)00104-9](http://dx.doi.org/10.1016/S0011-2240(02)00104-9).
  33. Fritz-Laylin LK, Prochnik SE, Ginger ML, Dacks JB, Carpenter ML, Field MC, Kuo A, Paredez A, Chapman J, Pham J, Shu S, Neupane R, Cipriano M, Mancuso J, Tu H, Salamov A, Lindquist E, Shapiro H, Lucas S, Grigoriev IV, Cande WZ, Fulton C, Rokhsar DS, Dawson SC. 2010. The genome of *Naegleria gruberi* illuminates early eukaryotic versatility. *Cell* 140:631–642. <http://dx.doi.org/10.1016/j.cell.2010.01.032>.
  34. Huranová M, Ivani I, Benda A, Poser I, Brody Y, Hof M, Shav-Tal Y, Neugebauer KM, Staněk D. 2010. The differential interaction of snRNPs with pre-mRNA reveals splicing kinetics in living cells. *J. Cell Biol.* 191:75–86. <http://dx.doi.org/10.1083/jcb.201004030>.
  35. Partikian A, Olveczky B, Swaminathan R, Li Y, Verkman AS. 1998. Rapid diffusion of green fluorescent protein in the mitochondrial matrix. *J. Cell Biol.* 140:821–829. <http://dx.doi.org/10.1083/jcb.140.4.821>.
  36. Hashimi H, Zimmer SL, Ammerman ML, Read LK, Lukeš J. 2013. Dual core processing: MRB1 is an emerging kinetoplast RNA editing complex. *Trends Parasitol.* 29:91–99. <http://dx.doi.org/10.1016/j.pt.2012.11.005>.
  37. Panigrahi AK, Zíková A, Dalley RA, Acestor N, Ogata Y, Anupama A, Myler PJ, Stuart KD. 2008. Mitochondrial complexes in *Trypanosoma brucei*: a novel complex and a unique oxidoreductase complex. *Mol. Cell. Proteomics* 7:534–545. <http://dx.doi.org/10.1074/mcp.M700430-MCP200>.
  38. Maslov D, Agrawal R. 2012. Mitochondrial translation in trypanosomatids, p 215–236. *In* Bindereif A (ed), *RNA metabolism in trypanosomes*. Springer, Berlin, Germany.
  39. Schnauffer A, Domingo GJ, Stuart K. 2002. Natural and induced dyskinetoplastic trypanosomatids: how to live without mitochondrial DNA. *Int. J. Parasitol.* 32:1071–1084. [http://dx.doi.org/10.1016/S0020-7519\(02\)00020-6](http://dx.doi.org/10.1016/S0020-7519(02)00020-6).